Geophysical Journal International

Geophys. J. Int. (2010) doi: 10.1111/j.1365-246X.2010.04586.x

On the amplitude of surface waves obtained by noise correlation and the capability to recover the attenuation: a numerical approach

Paul Cupillard* and Yann Capdeville

Département de sismologie, IPGP, 4 *place Jussieu,* 75252 *Paris Cédex* 05*, France. E-mail: paulcup@ipgp.jussieu.fr*

Accepted 2010 March 4. Received 2010 March 3; in original form 2009 September 24

SUMMARY

Cross-correlation of ambient seismic noise recorded by a pair of stations is now commonly recognized to contain the Green's function between the stations. Although traveltimes extracted from such data have been extensively used to get images of the Earth interior, very few studies have attempted to exploit the amplitudes. In this work, we investigate the information contained in the amplitudes and we probe the capability of noise correlations to recover anelastic attenuation. To do so, we carry out numerical experiments in which we generate seismic noise at the surface of a 1-D Earth model. One of the advantages of our approach is that both uniform and non-uniform distributions of noise sources can be taken into account. In the case of a uniform distribution, we find that geometrical spreading as well as intrinsic attenuation are retrieved, even after strong non-linear operations such as one-bit normalization and spectral whitening applied to the noise recordings. In the case of a non-uniform distribution of sources, the geometrical spreading of the raw noise correlations depends on the distribution, but intrinsic attenuation is preserved. For the one-bit noise and whitened noise correlations, the interpretation of observed amplitude decays requires further study.

Key words: Surface waves and free oscillations; Seismic attenuation; Computational seismology; Wave propagation.

1 INTRODUCTION

Recent developments have shown that the Green's function (GF) between two distant seismometers can emerge from the cross-correlation of a sufficient duration of seismic noise recorded at both seismometers (Shapiro & Campillo 2004). This fact provides new data of great interest for seismologists, because they enable imaging of Earth structure in aseismic regions. In most applications, the emerging signal is dominated by surface waves. Group-speeds on interstation paths are now widely measured and numerous high-resolution tomographic images have appeared over the last 5 years (e.g. Shapiro *et al.* 2005; Cho *et al.* 2007; Lin *et al.* 2007; Yang *et al.* 2007; Bensen *et al.* 2008; Stehly *et al.* 2009).

The emergence of the GF between two stations is possible because the noise sources create a spatially and temporally incoherent wavefield that carries, nevertheless, a small coherent part. This small coherent part is due to the sources that produce paths, which reach either one of the receivers via the other. A time-averaged correlation of noise recorded at these receivers enables recovery of this coherency. Prior to its use in seismology, this result was successfully applied in other fields such as helioseismology (Duvall *et al.* 1993) and ultrasonics (Lobkis & Weaver 2001; Weaver & Lobkis 2001, 2003). Many theoretical developments subsequently explained the phenomenon. Lobkis & Weaver (2001) were the first to describe the incoherent wavefield as a sum of equipartitioned modes and show that correlation of two records of such a field yields the GF. More recently, the wavefield was seen as an uncorrelated and isotropic mix of plane waves from all propagation direction (Weaver & Lobkis 2003). With this definition, Sánchez-Sesma & Campillo (2006) and Sánchez-Sesma *et al.* (2006) show that equipartitioning of the wavefield is a necessary condition for retrieving the exact GF. Other developments, based on an analogy with time-reversal experiments (Derode *et al.* 2003), the fluctuation-dissipation theorem (van Tiggelen 2003) or reciprocity (Wapenaar 2004), and stationary-phase derivation (Snieder 2004), also demonstrate the emergence of GFs from ambient noise correlations.

All these theories only take into account the case of uniformly distributed noise sources. Now, as Sánchez-Sesma & Campillo (2006) assess, 'an anisotropic flux as well as the absence of equipartition has to be considered to fully understand the limitations of the method'. Indeed, noise consistently observed in seismic records mainly comes from the oceans (Longuet-Higgins 1950) so that its distribution at the surface of the Earth clearly is non-uniform. Interest in the effects of such a distribution has recently grown (Weaver *et al.* 2009; Yao & van der Hilst 2009). In this paper, we study these effects by computing correlations of numerically generated seismic noise in an attenuating sphere. We also look at the influence on correlations of two processing techniques commonly applied to the noise records: one-bit normalization and spectral whitening

*Now at: Seismological Laboratory, University of California, Berkeley, CA 94720, USA. E-mail: paulcup@seismo.berkeley.edu

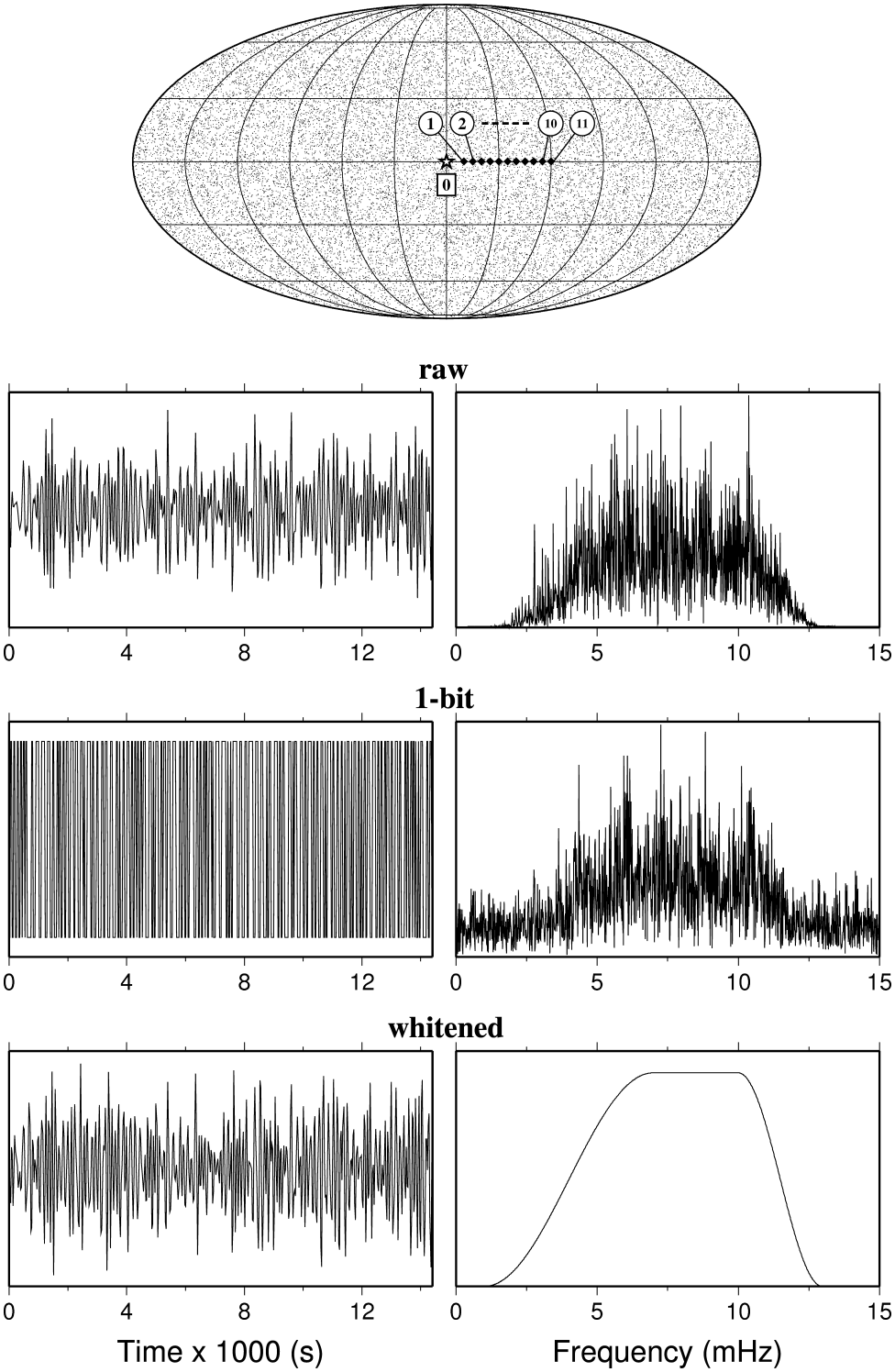

Figure 1. Top panel: source and receiver configuration of our first experiment. Stations $n = 1, \ldots, 11$ (black diamonds) are $(n + 1) \times 5^\circ$ far from station 0 (white star). Tiny dot pixels indicate the location of 24 000 noise sources (80 realizations) randomly distributed on the surface of the Earth. Bottom panel: an example of noise recorded at station 0 is presented (left panel) for the three different noise processing we consider (raw, one-bit normalization and whitening). We also plot the amplitude spectrum of these recordings (right panel).

(Bensen *et al.* 2007). One-bit normalization is a procedure for reducing the weight of the earthquakes that inevitably lie in seismic records. It consists of retaining only the sign of the raw signal by replacing all positive amplitudes with a 1 and all negative amplitudes with a -1. Spectral whitening is often practiced as well to enhance frequencies with low amplitude. Other noise-processing techniques, not studied in this paper, can be found in Bensen *et al.* (2007).

Traveltimes of ambient noise correlations have been extensively used so far. In this paper, we want to probe the information contained in the amplitude of such data. To do so, we compare our

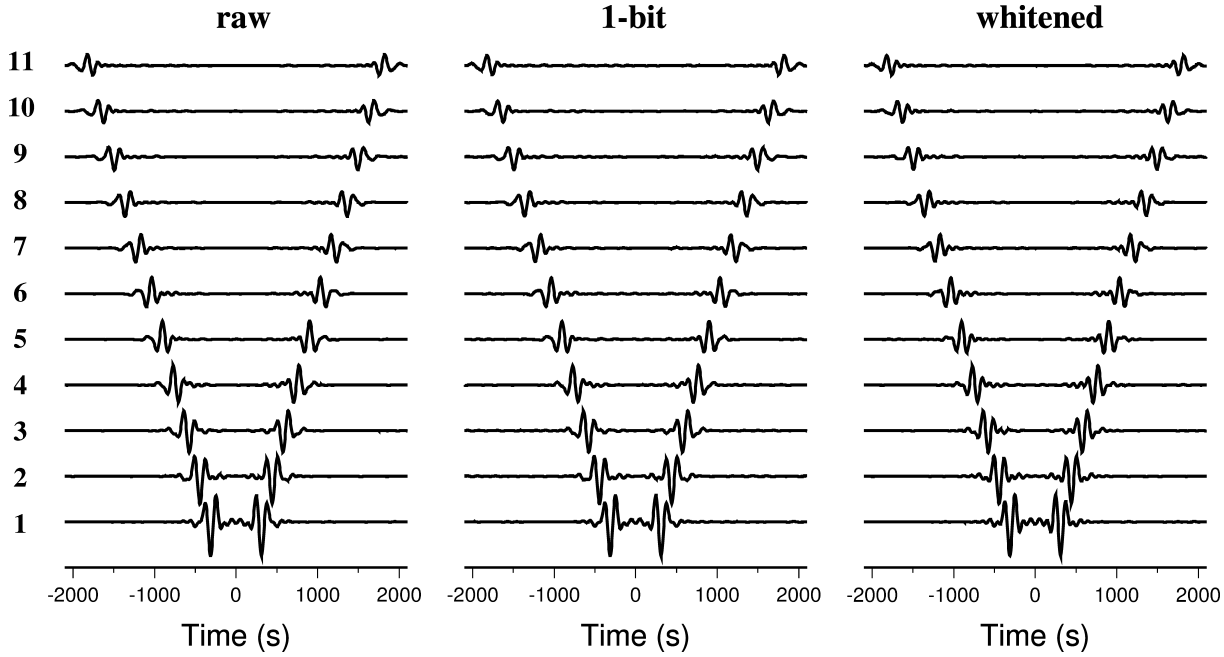

Figure 2. Cross-correlations between the vertical displacement recorded at 0 and the vertical displacement at n (numbers on the left) in the case of a uniform distribution of noise sources. Three data sets are presented corresponding to the three different noise processing investigated in this work: raw, one-bit normalization and whitening.

synthetic correlations with the full waveforms of exact GFs computed with a normal-mode summation technique. The behaviour of our reconstructed Rayleigh waves with respect to the attenuation (geometrical spreading and anelasticity) is addressed by carefully analysing the amplitude decay with increasing interstation distance. Our results are then discussed in the context of previous studies that deal with the same topic (Larose *et al.* 2007; Gouédard *et al.* 2008; Matzel 2008; Prieto *et al.* 2009).

2 UNIFORM DISTRIBUTION OF NOISE SOURCES

2.1 Experimental setup

We compute synthetic noise at the surface of a spherical attenuating Earth to mimic the continuous oscillations that are consistently observed in seismic records and commonly considered to come from interactions between the atmosphere, ocean and seafloor. Such oscillations do not have a flat amplitude spectrum; two peaks generally are present around 14 and 7 s period, which are referred to as primary and secondary microseism, respectively (Longuet-Higgins 1950; Friedrich *et al.* 1998; Stehly *et al.* 2006). Moreover, at longer periods (150–500 s), the so-called Earth 'hum' is observed (Nawa *et al.* 1998; Rhie & Romanowicz 2004; Kedar & Webb 2005). In this work, we do not try to simulate the complex mechanisms, which produce this kind of spectra. We will consider simple noise sources with flat spectra in a specified frequency band.

To create our synthetic noise, we randomly position 300 sources on the surface of the Earth. For each spatial component of each source, we generate a 24-hr time-series with random phase and flat spectrum filtered between 100 and 150 s. Using normal-mode summation (e.g. Woodhouse & Girnius 1982) in the Preliminary Reference Earth Model (Dziewonski & Anderson 1981), the effect of all the sources is computed at 12 stations $n = 0, \ldots, 11$. All the stations are located on the equator. We distinguish receiver $n = 0$ at longitude 0° from the other receivers $n = 1, \ldots, 11$ at longitude $(n + 1) \times 5^\circ$ (Fig. 1). The correlations between the vertical displacement recorded at 0 and the vertical displacement at the other stations are computed. That is the result of what we call a 'realization'. Because a single realization is not enough to get a good convergence, we perform 5120 realizations (we use 64 processors; each of them computes 80 realizations; the total number of sources then is 1 536 000). Stacking all the realizations, we obtain the waveforms represented in Fig. 2.

Three different cases are studied corresponding to different processes applied to the noise records: (1) raw noise (no treatment is done); (2) one-bit noise (meaning that only the sign of the waveforms is considered); (3) whitened noise (meaning that the spectral amplitudes of each record are set to 1 in the chosen frequency band). One-bit normalization is widely used to attenuate earthquake signals from real seismic records (e.g. Shapiro & Campillo 2004; Yao *et al.* 2006) or enhance codas relative to first arrivals (e.g. Campillo & Paul 2003; Paul *et al.* 2005). Although there is no earthquake in our experiment, we apply a one-bit normalization because we want to investigate the effect of such a strong non-linear operation on the amplitude of cross-correlations. Frequency whitening is another non-linear operation frequently used to prepare noise prior to correlation. The whitening we adopt in this work is very aggressive: the amplitude spectrum of the original raw noise is replaced by a boxcar smoothed using a cosine-taper. This procedure has been used in previous studies (e.g. Stehly *et al.* 2009). Less aggressive and more sophisticated whitenings are described in Bensen *et al.* (2007).

Fig. 1 shows a 4-hr noise record processed in the three ways mentioned earlier. The effect of the one-bit normalization is clearly visible in the time domain, whereas the whitening effect appears in the frequency domain. Each process provides a set of correlations (Fig. 2). All the correlations are symmetric: the waveforms at negative and positive times are the same in shape and amplitude. This is because the energy flux is the same from station 0 to station n

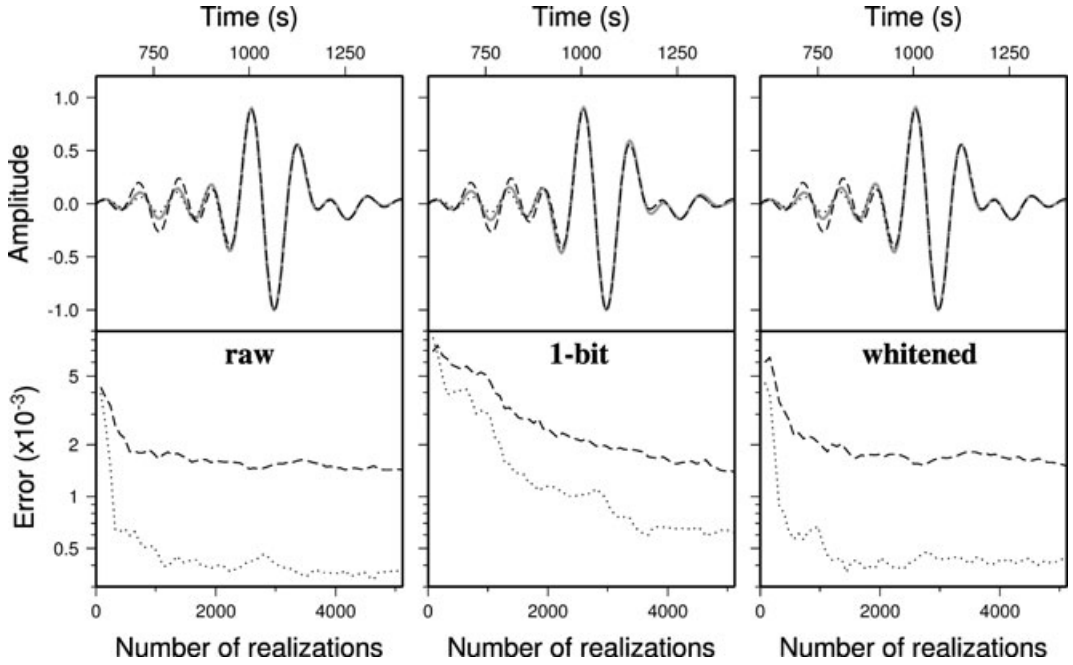

Figure 3. Top panel: for each process applied to the noise records (raw, one-bit normalization and whitening), the correlation between stations 0 and 6 (grey line) is compared with the corresponding Green's function (dashed line) and the fundamental mode (dotted line). To focus on the Rayleigh wave, we use a 800 s time window centred on $t = 1000$ s. The correlations are obtained using 1 536 000 noise sources (5120 realizations). These sources are uniformly distributed on the surface of the Earth. Bottom panel: the dashed (dotted) line is the error between the correlation and the Green's function (the fundamental mode) with respect to the number of realizations. For every process, we converge to a small and stable error. Moreover, the error from the Green's function is systematically larger than the error from the fundamental mode.

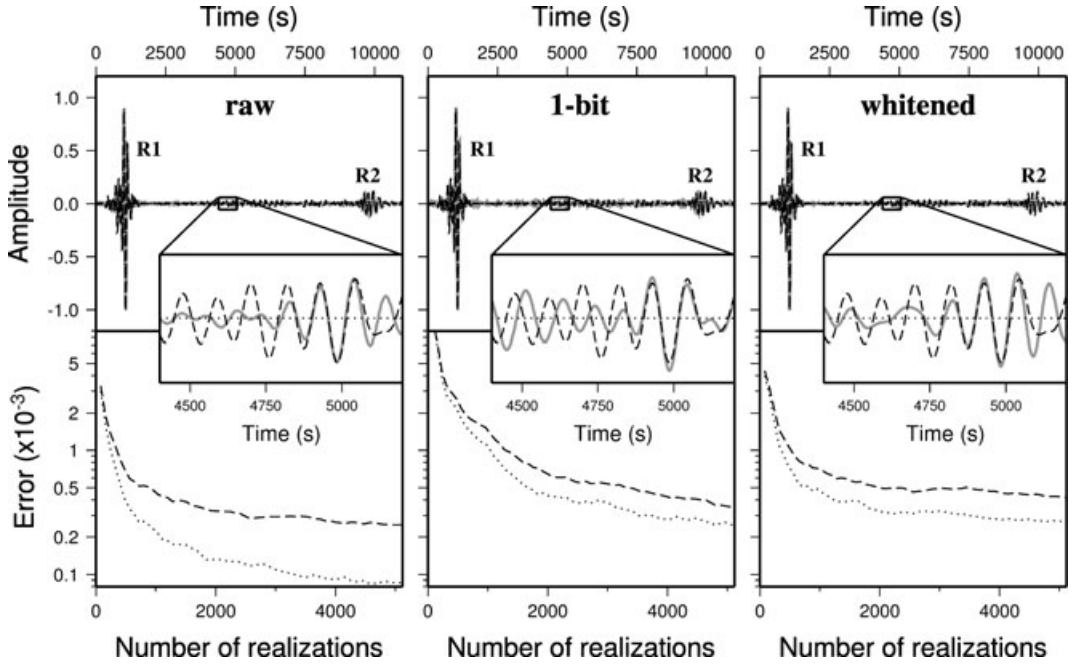

Figure 4. Same as Fig. 3 but the time window is now 11 000 s wide. R1 (the Rayleigh wave travelling along the short arc of the great circle) and R2 (the Rayleigh wave from the long arc) are both visible. Zooming in on a part of the signal where the energy of the fundamental mode is negligible shows that the correlation can retrieve some, but not all, overtones. In the chosen time window, the error from the fundamental mode is very slightly smaller than the error from the Green's function. After a sufficient number of realizations, the two errors are small and stable for the three noise processing.

(negative part) than from n to 0 (positive part). As expected, the arrival time of the wave packets increases as interstation distance becomes larger. On the contrary, the amplitude decreases as interstation distance increases. This decay will be studied more precisely at the end of Section 2.2.

2.2 Comparison with the Green's function

The Green's tensor between two stations in a laterally homogeneous sphere can be easily computed using normal-mode summation. Following Woodhouse & Girnius (1982), we can write the vertical

displacement G_{nm} at a station m due to a vertical Dirac delta function at another station n as a function of time t

$$G_{nm}(t) = \sum_k a_k(n) u_k(m) \mathrm{e}^{\mathrm{i}\omega_k t}, \quad (1)$$

where u_k and ω_k are the eigenfunctions and eigenfrequencies of the Earth model, and a_k are the excitation coefficients due to the vertical Dirac delta function. Using this equation, we are able to calculate the reference GFs against which we can compare our correlations. To make the comparison possible, we have to differentiate the correlations in time and correct them for a source term, which is the power spectral density of the noise, recorded at one station. Indeed, different authors (Lobkis & Weaver 2001; Snieder 2004; Colin de Verdière 2006; Sánchez-Sesma *et al.* 2008) have demonstrated that, in 3-D, we have

$$\mathrm{i}\omega C_{nm}(\omega) \propto |S_n(\omega)|^2 G_{nm}(\omega), \quad (2)$$

where C_{nm} is the side of the correlation between n and m that corresponds to the noise going from n to m, ω is the angular frequency and S_n is the noise recorded at n. $||$ denotes the modulus of a complex quantity.

Fig. 3 shows a comparison of the corrected correlations from station 6 with the corresponding GF on the one hand, and with the fundamental mode (eq. 1 restricted to $k \in \{\text{fundamental mode}\}$) on the other hand. We chose a 800 s time window centred on $t = 1000$ s to focus on the Rayleigh wave. For each kind of noise processing (raw, one-bit normalization and whitening), the correlation fits both the GF and the fundamental mode very well. Nevertheless, the computation of the mean square deviation of the full waveform (hereafter referred to as the error) shows that the fit is a little better for the fundamental mode. This is mainly due to the discrepancy between the GF and the correlation in the 650–850 s time window: it looks like the correlation is not able to retrieve overtones. This is confirmed in Fig. 4. This figure shows the same comparison as in Fig. 3 but using a much larger time window (11 000 s). Zooming in a part of the signal that has overtones only (the curve of the fundamental mode is equal to zero), we see that some of them are recovered whereas some others are not. This means that the correlation of a seismic wavefield produced by noise sources, which are uniformly distributed on the surface of a 1-D Earth, does not perfectly converge to the GF. The convergence of such a correlation towards the fundamental mode is better (this is visible on both Figs 3 and 4) but is not perfect either. Nervertheless, the quality of our reconstructed Rayleigh waves is very good for our purpose.

The reason why some overtones are not retrieved in our correlations is that there are no noise sources at depth in our experiment. Including such sources enables to recover all the overtones, as shown in Fig. 5(a). This figure presents the raw noise correlation between stations 0 and 6 when using sources everywhere in the medium. As done before, we use two time windows to compare this correlation with the GF and the fundamental mode. For each of these two windows, we compute the error as a function of realizations. Because a good convergence requires more realizations than in the case of sources distributed on the surface, we performed 9600 realizations. It is clear that the correlation now fits the GF better than the fundamental mode. Nevertheless, the error between the correlation and the GF stabilizes to a non-zero value. This is because the amplitudes are not correctly retrieved (see the zoom window in the overtones). As stated by Snieder (2007), getting an equipartitioned wavefield (and thus an accurate reconstruction of the GF) in an attenuating medium requires a source excitation that is proportional to the local dissipation rate. We do not use such a particular excitation here so

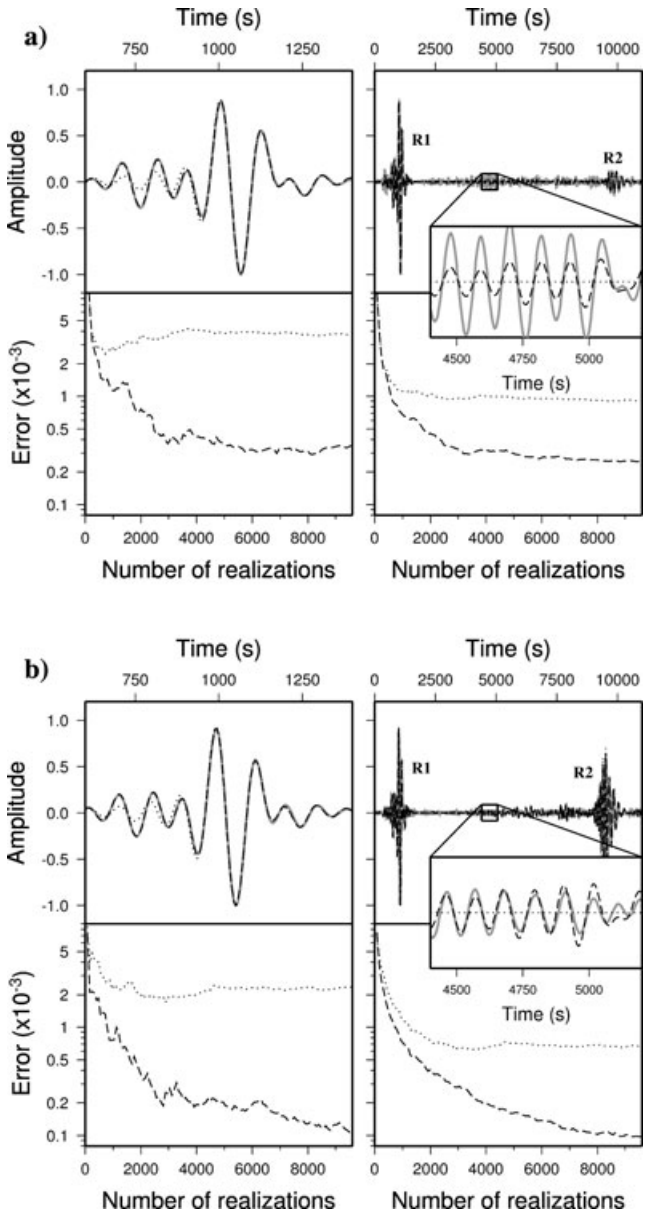

Figure 5. Raw noise correlation between stations 0 and 6 (grey line) emerging from a uniform distribution of noise sources in the interior of the Earth. Two different experiments are carried out: one in an attenuating medium (a) and one in a lossless medium (b). The result of each experiment is compared with the GF (dashed line) and the fundamental mode (dotted line) using two different time windows. The error as a function of realizations is computed for each of these two windows. In both experiment, the correlation fits the GF better than the fundamental mode. In the attenuating Earth, the amplitudes are not very well recovered, so the error between the correlation and the GF stabilizes to a non-zero value. In the lossless Earth, the GF is very well retrieved.

we do not get the exact GF. We check that the anelasticity is indeed the cause of the discrepancy between the GF and the correlation by performing the same experiment in a lossless medium. The result shows that the GF is accurately recovered in this case (Fig. 5b). Similar observations are found for one-bit noise and whitened noise correlations.

The purpose of this paper is to study the amplitude of surface waves reconstructed by noise correlation in the context of noise sources located on the surface of the Earth. Therefore, we do not

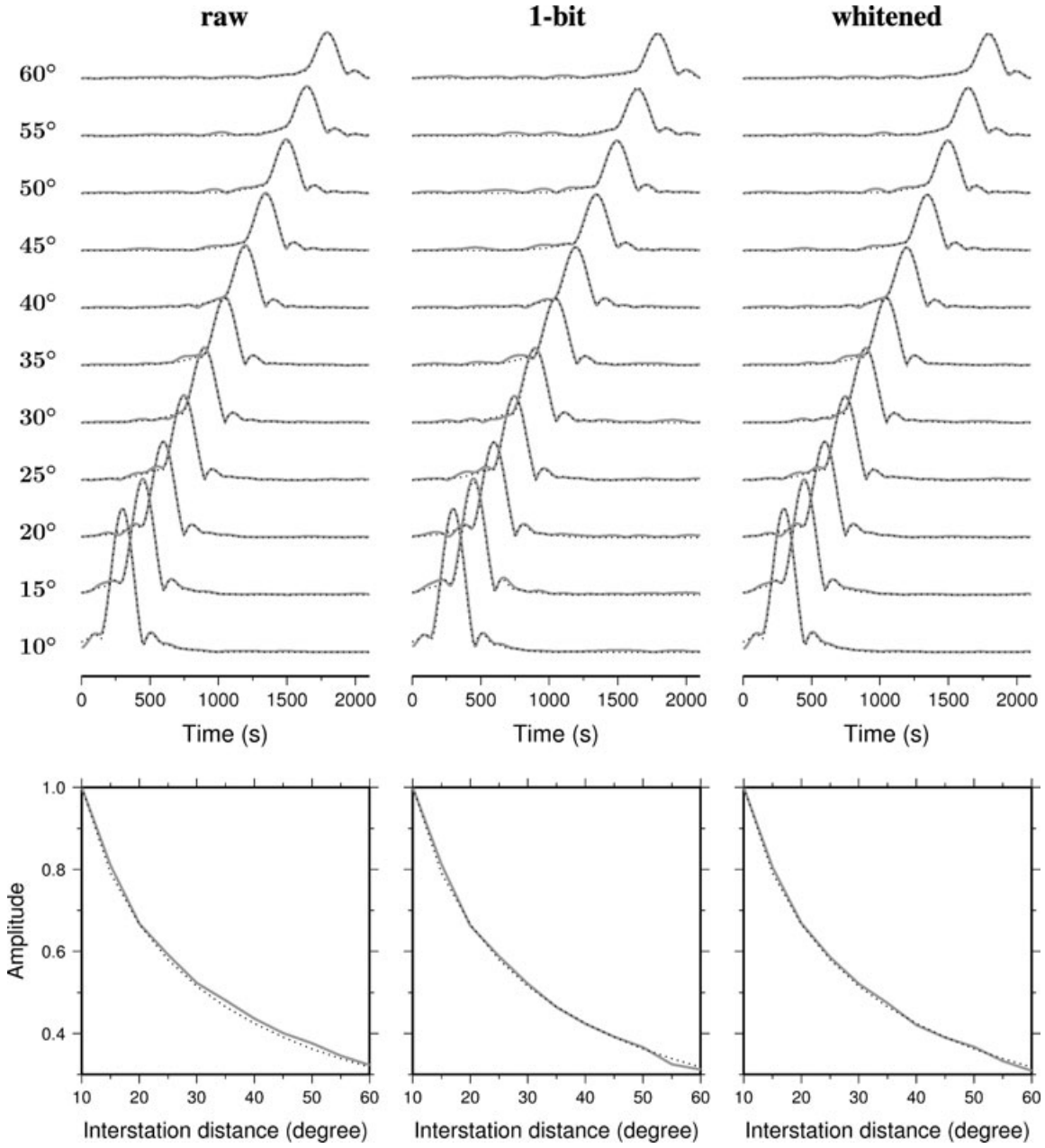

Figure 6. Comparison of the amplitude decay of the envelope of the correlations (grey line) with their corresponding fundamental mode (dotted line) in the case of a uniform distribution of noise sources. Top panel: The waveforms from the three processes (column) and all the stations (row) are presented. Bottom panel: The maximum of amplitude is plotted as a function of interstation distance.

consider the correlations obtained using sources at depth in what follows. As shown in Fig. 3, the quality of the Rayleigh waves obtained using sources on the surface is very good. Because the convergence of these waves towards the fundamental mode is better than the convergence towards the GF, we choose the fundamental mode as the reference in what follows and we compare the amplitude decay of our reconstructed Rayleigh waves with the decay of the fundamental mode (Fig. 6). We match the amplitude maximum of the signals at station 1 so we can see how the relative amplitudes evolve as interstation distance increases. We use the envelope of the signals because it is closely related to the energy, and thus to the attenuation (Aki & Richards 1980). We observe that the signal envelopes are very similar for each interstation distance and regardless of the noise processing. Plotting the amplitude maximum as a function of interstation distance, we see that the decay of the correlation is the same as that of the fundamental mode. This means that, in the context of a uniform distribution of noise sources on the surface of a radially symmetric Earth, cross-correlations contain geometrical spreading as well as intrinsic attenuation, even after applying strong non-linear operations on the amplitude of the noise like one-bit normalization and frequency whitening. As the Rayleigh wave Green's function is highly dominated by the fundamental mode, the results and the conclusion would be the same if considering the GF as the reference.

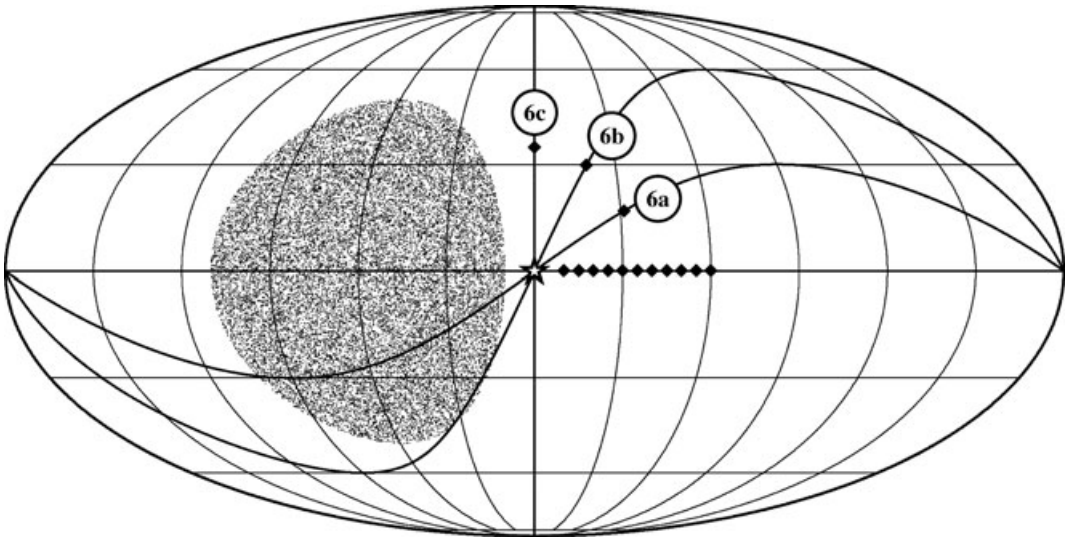

Figure 7. Configuration of the second experiment. Tiny dot pixels indicate the location of 24 000 noise sources (80 realizations). We see that all the sources belong to a 50°-radius patch centred on the equator at longitude −60°. Again, we use station 0 (star) and stations $n = 1, \ldots, 11$ (diamonds) as introduced in Fig. 1. We add three new stations (6*a*, 6*b* and 6*c*) to study the anisotropy of the energy flux produced by such a distribution of noise sources.

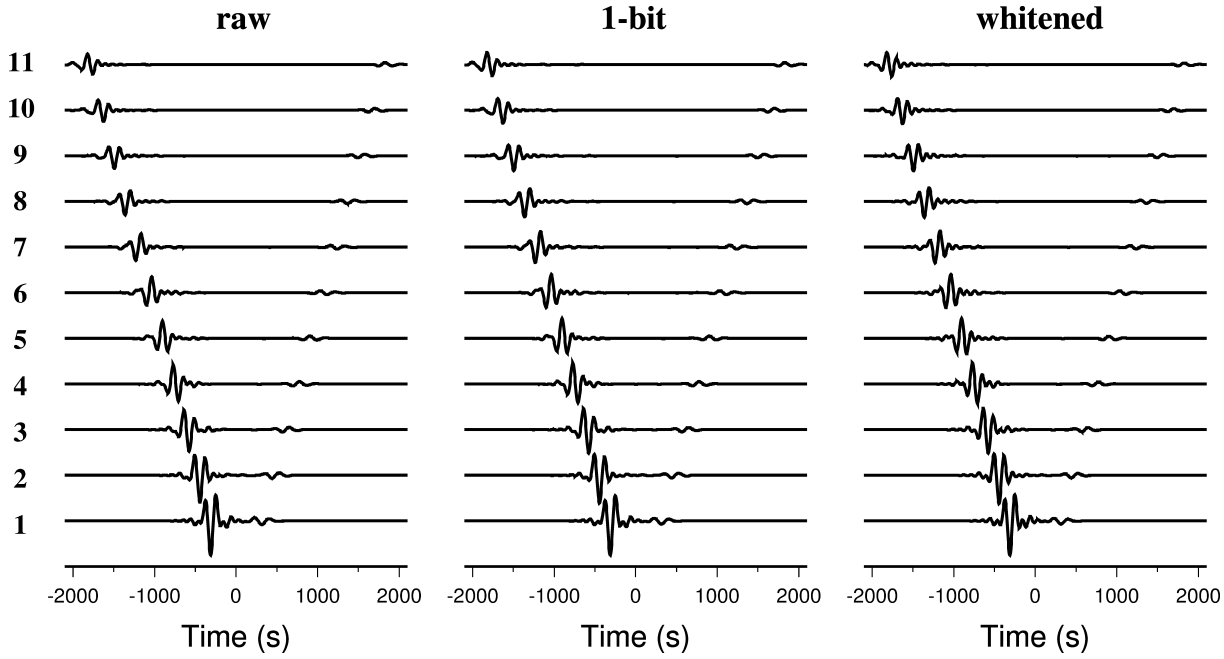

Figure 8. Cross-correlations between the vertical displacement recorded at 0 and the vertical displacement at n (numbers on the left) in the case of noise sources distributed in a big patch.

3 NOISE SOURCES DISTRIBUTED IN A BIG PATCH

3.1 Experimental setup

It is important to study the case of a non-uniform distribution of sources because seismic noise in the Earth mainly comes from the oceans and is therefore non-uniformly distributed. Such a distribution produces an anisotropic energy flux that is difficult to consider analytically and, therefore, has never been clearly taken into account. We probe the effects of wavefield inhomogeneity, by repeating the same experiment as the one in the previous section, except that the noise sources are now confined in a 50°-radius cap on the surface of the sphere. The centre of this cap is on the equator at longitude −60° (Fig. 7). Reducing the source location area and keeping the same number of realizations increases the source density. To investigate the impact of our space-limited 'noisy' area on cross-correlations, we use again a line of 12 stations ($n = 0, \ldots, 11$) along the equator. As the azimuths from station 0 are not all equivalent with respect to the patch of noise sources, we add three new stations that are not on the equator, 35° far from station 0 (as station 6 is), and call them 6*a*, 6*b* and 6*c*. They lie at an azimuth of 60°, 30° and 0° from receiver 0.

Fig. 8 shows the correlations between the displacement recorded at station 0 and the displacement from the other stations positioned

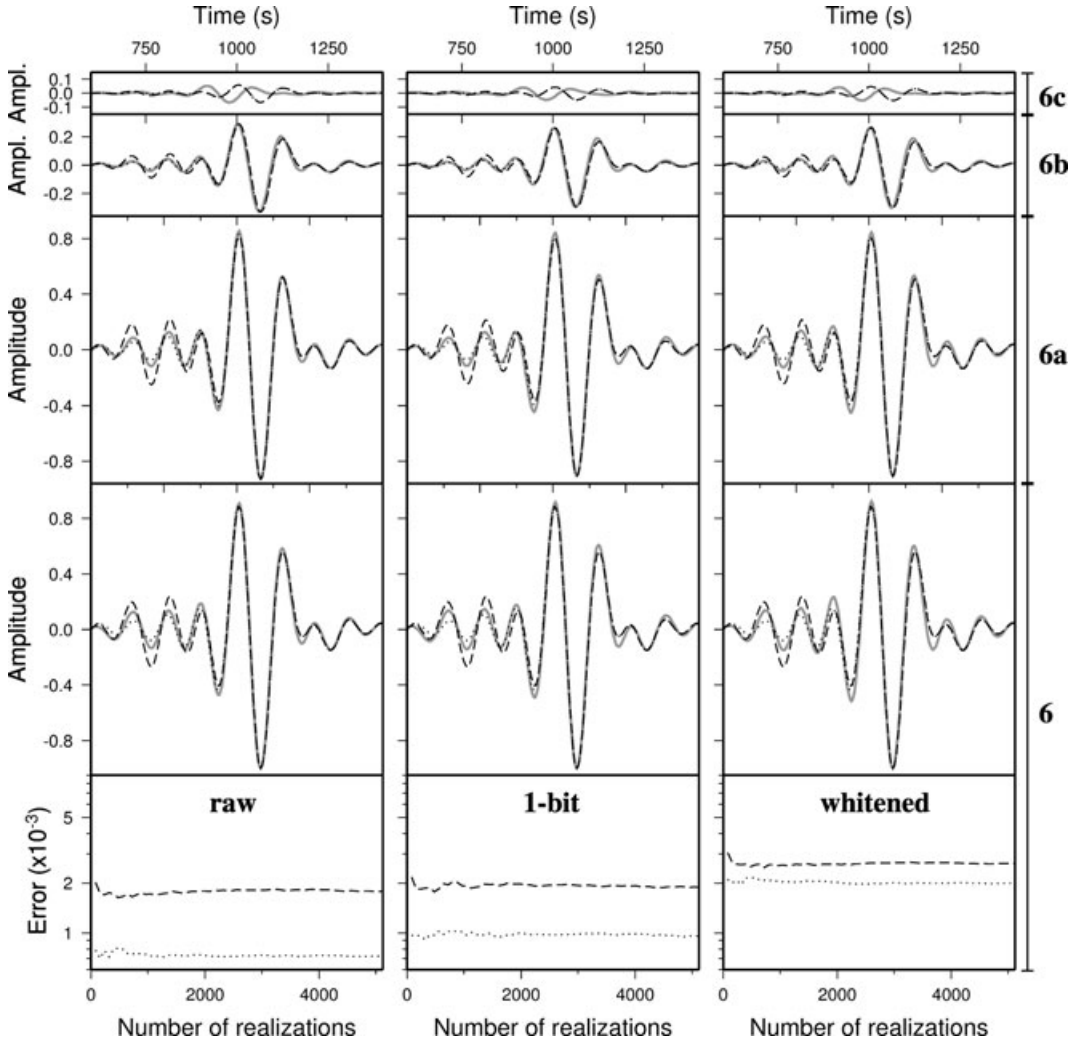

Figure 9. The correlations (grey line) from stations 6*c*, 6*b*, 6*a* and 6 (from the top to the bottom) are compared with the Green's function (dashed line) and the fundamental mode (dotted line) which are the same for the four stations because these latter are all 35° far from station 0. The relative amplitude of the correlations is preserved (and so we adapt the Green's function and the fundamental mode to match the amplitude of the correlations). For station 6, we also plot the convergence as we did in Fig. 3.

on the equator ($n = 1, \ldots, 11$). Strong asymmetry appears at all stations and for all processes applied to the noise. This is due to the anisotropy of the energy flux: the energy going from n to 0 is much lower than the energy going from 0 to n. This effect has been reported by many authors working on real data (Shapiro & Campillo 2004; Paul *et al.* 2005; Stehly *et al.* 2006; Yao *et al.* 2006; Nishida & Fukao 2007; Bensen *et al.* 2008). In the following, we will only consider waveforms at negative times (emerging from the noise going from 0 to n). We observe that their amplitude decreases as interstation distance increases. We will study this amplitude decay in the next section.

3.2 Comparison with the Green's function

Using eq. (2), we process our correlations to compare them with the GF. Fig. 9 shows the Rayleigh wave from station 6. As we did before in Fig. 3, we consider the fit to the GF as well as the fit to the fundamental mode. Plotting the error as a function of the number of realizations, we observe that the correlation fits the fundamental mode better than the GF. This is true for all three processes applied to the noise. We notice that the error becomes stable faster than it did in the previous experiment (Fig. 3). This is simply because the density of sources in the coherent zone, which is the vicinity of the great circle passing through the two stations 0 and 6 (Snieder 2004; Roux *et al.* 2005), is higher in the current experiment. We also notice that the final errors we get are larger than before. This means that the wavefield produced by the current distribution of noise sources is less equipartitioned than the wavefield due to a uniform distribution. Nevertheless, the quality of the reconstructed signal is satisfactory.

Fig. 9 also shows the correlations from stations 6*a*, 6*b* and 6*c*. The relative amplitude of these correlations has been preserved to clearly show that the energy flux is now anisotropic. The amplitude of the reconstructed signal increases with increasing the azimuth. This is because the number of noise sources in the coherent zone is not the same in all azimuths. There are no sources on the great circle defined by 0 and 6*c* (azimuth = 0°, cf. Fig. 7) so the correlation from 6*c* has a very small amplitude. On the contrary, the number of noise sources is high for stations 6 and 6*a* (azimuth = 90° and 60°, respectively) so the corresponding correlations have a large amplitude.

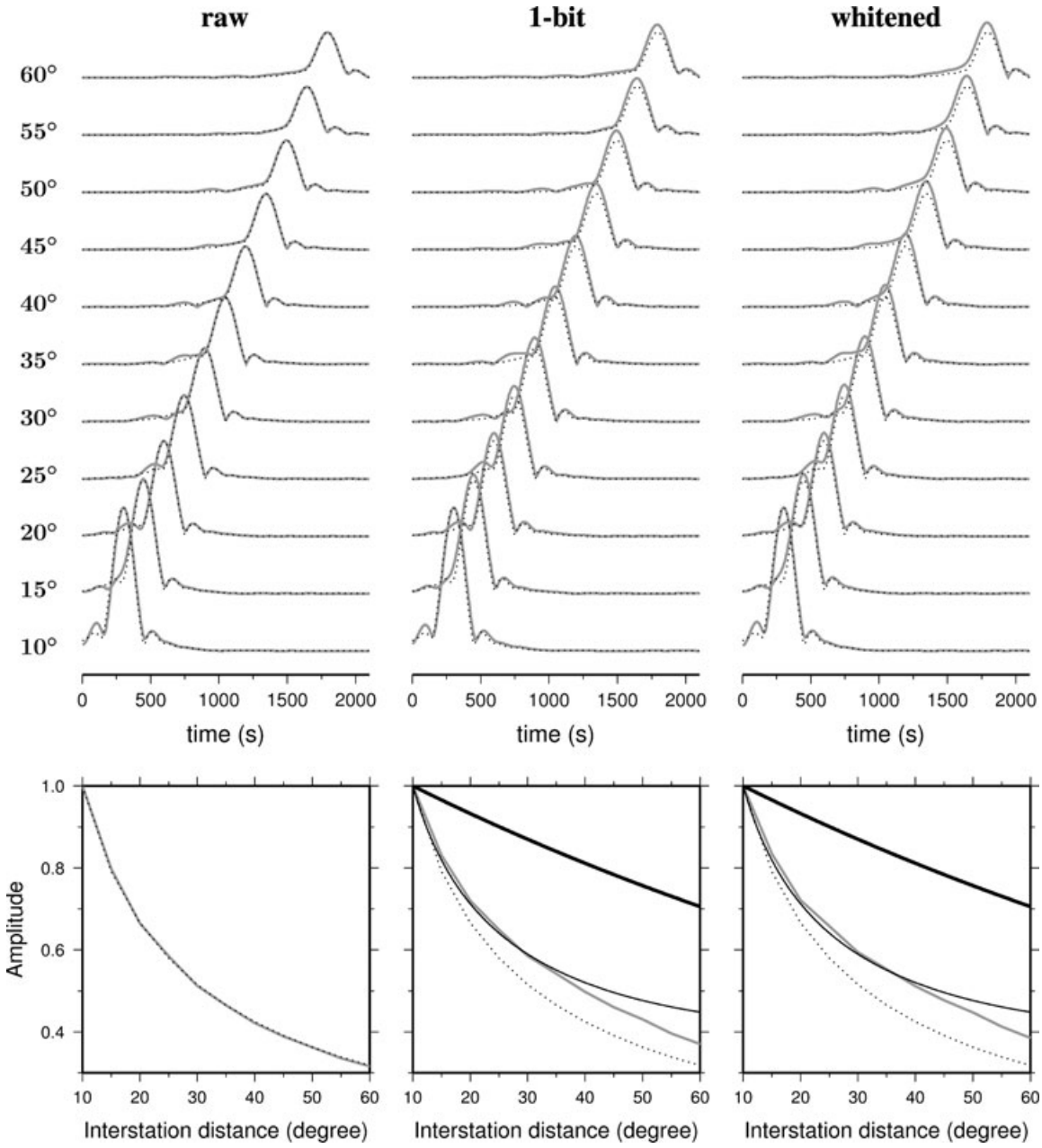

Figure 10. Comparison of the amplitude decay of the envelope of the correlations (grey line) with their corresponding fundamental mode (dotted line) in the case of noise sources distributed in a big patch. Top panel: The waveforms from the three processes (column) and all the stations on the equator (row) are presented. Bottom panel: The maximum of amplitude is plotted as a function of interstation distance. The decay of the one-bit and the whitened noise correlations does not fit the decay of the fundamental mode. It also fits neither geometrical spreading (thin black line) nor intrinsic attenuation (thick black line).

Besides, we note that the phase of the correlation from station 6*c* has nothing to do with the GF. This is because the noise sources that contribute to the emergence of this correlation are far from the vicinity of the great circle path resulting in erroneous traveltimes. This effect is not explicitly discussed but is substantially contained in the theoretical development of Roux *et al.* (2005). It has been also observed on real data (Stehly *et al.* 2007; Gouédard *et al.* 2008).

We now look at the amplitude decay of the correlations obtained from stations located at the equator. We compare the envelope of these correlations with the envelope of the fundamental mode and we plot the maximum of these envelopes as a function of interstation distance (Fig. 10). As was the case in the previous experiment, the decay of the raw noise correlation is the same as that of the fundamental mode. However, for the one-bit and the whitened noise correlations, this is no longer true; the amplitude decay corresponding to these two processes is less steep than the decay of the fundamental mode. We also plot the two terms that correspond to the two different attenuation processes. Writing the amplitude spectrum of the GF restricted to fundamental mode between station 0 and station n as

$$\left|G_{0n}^{k\in fund}(\omega)\right| \propto \frac{1}{\sqrt{\sin(d_n)}} \exp\left[-\frac{\omega d_n}{2c(\omega)Q(\omega)}\right], \tag{3}$$

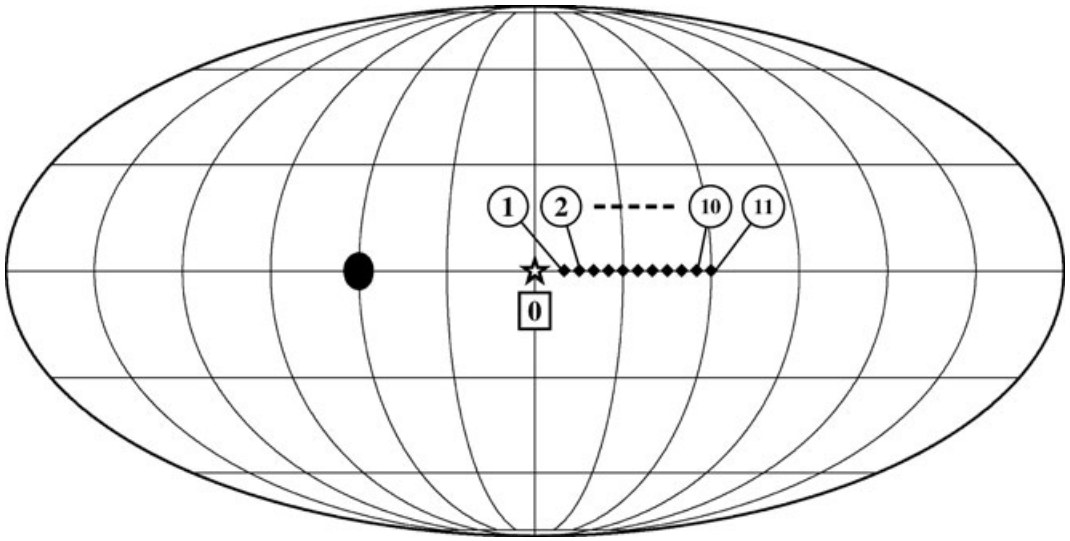

Figure 11. Configuration of the third experiment. The big black dot indicates the cap where the noise sources are. All the sources belong to a 5°-radius patch centred on the equator at longitude −60°. We use twelve receivers on the equator: station 0 (star) and stations $n = 1, \ldots, 11$ (diamonds).

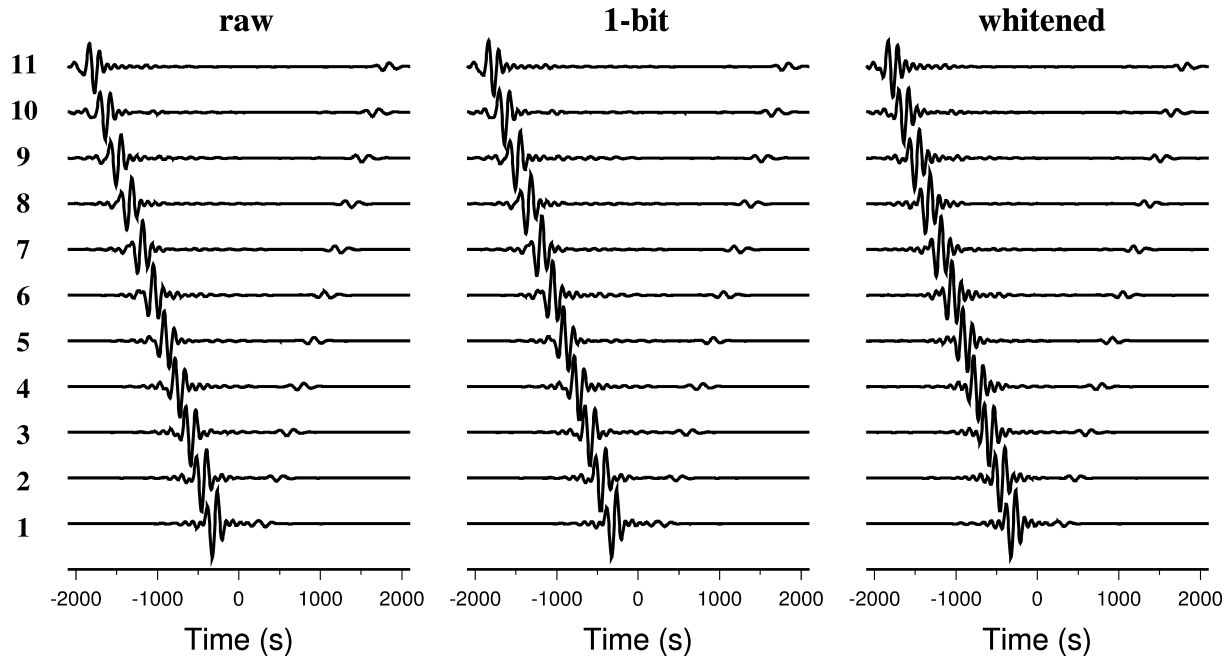

Figure 12. Cross-correlations between the vertical displacement recorded at 0 and the vertical displacement at n (numbers on the left) in the case of noise sources distributed in a small patch.

where d_n is the angular distance between the two stations, c is the Rayleigh wave speed and Q is the quality factor of the medium, we recognize the first term of the product to be the geometrical spreading and the second term to be the intrinsic attenuation. The plot of these two terms in Fig. 10 shows that they both provide a significant contribution to the amplitude of the fundamental mode. The amplitude decay of the one-bit and the whitened noise correlations does not fit any of the two terms. One can reasonably think that the one-bit and the whitened data sets both contain information on the intrinsic attenuation of the medium. However, in the case of the distribution of noise sources studied in this section, it is not possible to treat these data sets as one treats usual records (such as earthquake records) to extract the intrinsic attenuation.

4 NOISE SOURCES DISTRIBUTED IN A SMALL PATCH

4.1 Experimental setup

To investigate extreme source inhomogeneity, one last experiment is carried out. We now distribute the noise sources in a 5°-radius patch centred on the equator at longitude −60° (Fig. 11). The 12-stations line along the equator is used again to compute correlations. As expected, the obtained waveforms are asymmetric (Fig. 12). Moreover, for all three treatments used to process the noise records, we observe that the amplitude decay of the correlations with increasing interstation distance looks less strong than observed in the two

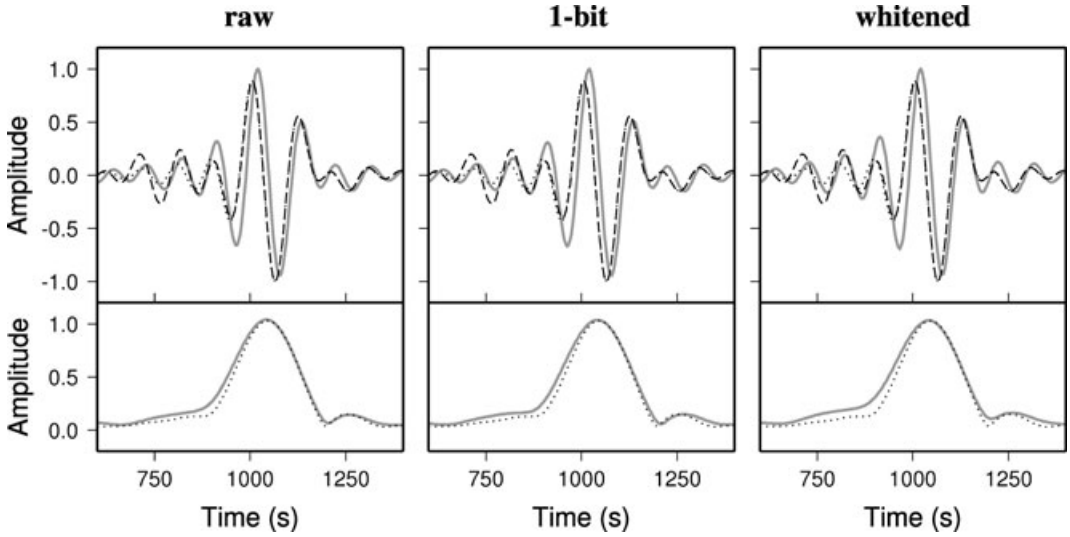

Figure 13. The correlations (grey line) from station 6 are compared with the Green's function (dashed line) and the fundamental mode (dotted line). The noise sources producing the wavefield that we correlate are confined in a small patch. Top panel: A $\pi/4$ phase shift appears between the correlations and the two other curves. Bottom panel: The phase shift is no longer visible when using the envelope of the signals.

previous experiments. We will carefully look at this variation of amplitude in the next section.

4.2 Comparison with the Green's function

There is substantial misfit between the corrected correlation (eq. 2) from station 6 and the corresponding GF and fundamental mode predictions (Fig. 13). This misfit mainly comes from a $\pi/4$ phase shift, which is known to make phase velocity measurements from noise correlations very ambiguous (Harmon *et al.* 2008). Indeed, in the general case (i.e. the case of any given distribution of noise sources), it is not clear whether the extracted GF is 2-D or 3-D. The main difference between these two kinds of function precisely is a $\pi/4$ shift (Aki & Richards 1980; Sánchez-Sesma & Campillo 2006). In spite of the ambiguity, Yao *et al.* (2006) and Lin *et al.* (2008) have succeeded in extracting phase velocity maps from noise correlations. In this work, the $\pi/4$ phase shift is not a problem because we use the envelope of the signals to study variations in amplitude. As shown in Fig. 13, the envelope of the correlation is very similar to the envelope of the fundamental mode, confirming the robustness of group velocity measurements from noise correlations.

Fig. 14 shows how the amplitude of the correlations decreases with increasing interstation distance. For each process, the decay is very different from the decay of the fundamental mode. We think this difference could be due to different geometrical spreading. Indeed, the small patch can be viewed as a point source providing a wavefield that is coherent between station 0 and station n (all the paths going through 0 also go through n) such that

$$|C_{0n}(\omega)| = |S_0(\omega)||S_n(\omega)| \tag{4}$$

with

$$|S_0(\omega)| = \frac{A(\omega)}{\sqrt{\sin(D)}} \exp\left[-\frac{\omega D}{2c(\omega)Q(\omega)}\right] \tag{5}$$

and

$$|S_n(\omega)| = \frac{A(\omega)}{\sqrt{\sin(D+d_n)}} \exp\left[-\frac{\omega(D+d_n)}{2c(\omega)Q(\omega)}\right], \tag{6}$$

where A is the amplitude spectrum of the signal at the source and D is the distance in degrees between station 0 and the point source (60° in our simulation). We here assume that noise propagates as surface waves. Substituting eqs (5) and (6) in eq. (4) gives

$$|C_{0n}(\omega)| = \frac{\alpha(\omega)}{\sqrt{\sin(D+d_n)}} \exp\left[-\frac{\omega d_n}{2c(\omega)Q(\omega)}\right], \tag{7}$$

where $\alpha = |S_0(\omega)|^2\sqrt{\sin(D)}$ is a constant with respect to d_n. From expression (7), we see that intrinsic attenuation acts in the correlation as it does in the GF. This is not true for geometrical spreading: the term corresponding to this attenuation in eq. (7) is different from the one in eq. (3). Correcting the amplitude decay of the raw noise correlation using $\sqrt{\sin(D+d_n)/\sin(d_n)}$ confirms our theory: the decay of the fundamental mode is retrieved, meaning that raw noise correlations can be used to measure the attenuation of the medium if the distribution of noise sources is known. This is a major result because it shows that meaningful information can be extracted from the amplitude of raw noise correlations. The same correction applied to the one-bit and the whitened noise correlations does not enable to recover the good amplitude decay. Similarly to the previous experiment, further work is needed to understand what these decays exactly contain.

5 DISCUSSION AND CONCLUSIONS

Records of synthetic noise computed in PREM using the normal-mode summation method enabled us to investigate different features of waveforms obtained by noise correlation. We paid particular attention to the relative amplitude of such waveforms. We find that this amplitude strongly depends on the distribution of noise sources and the processing applied to the noise records prior to correlation. If the sources are uniformly distributed on the surface of the Earth, then the amplitude decay we observe along a line of stations is the same as the decay of the Rayleigh wave Green's function. This is true regardless of the noise processing technique. If the distribution is not uniform, then the amplitude decay depends on the processing. Whereas raw noise correlations contain the intrinsic attenuation of the medium and geometrical spreading that is determined by the position of the noise sources, one-bit noise and whitened noise correlations result in decays that do not fit that of the

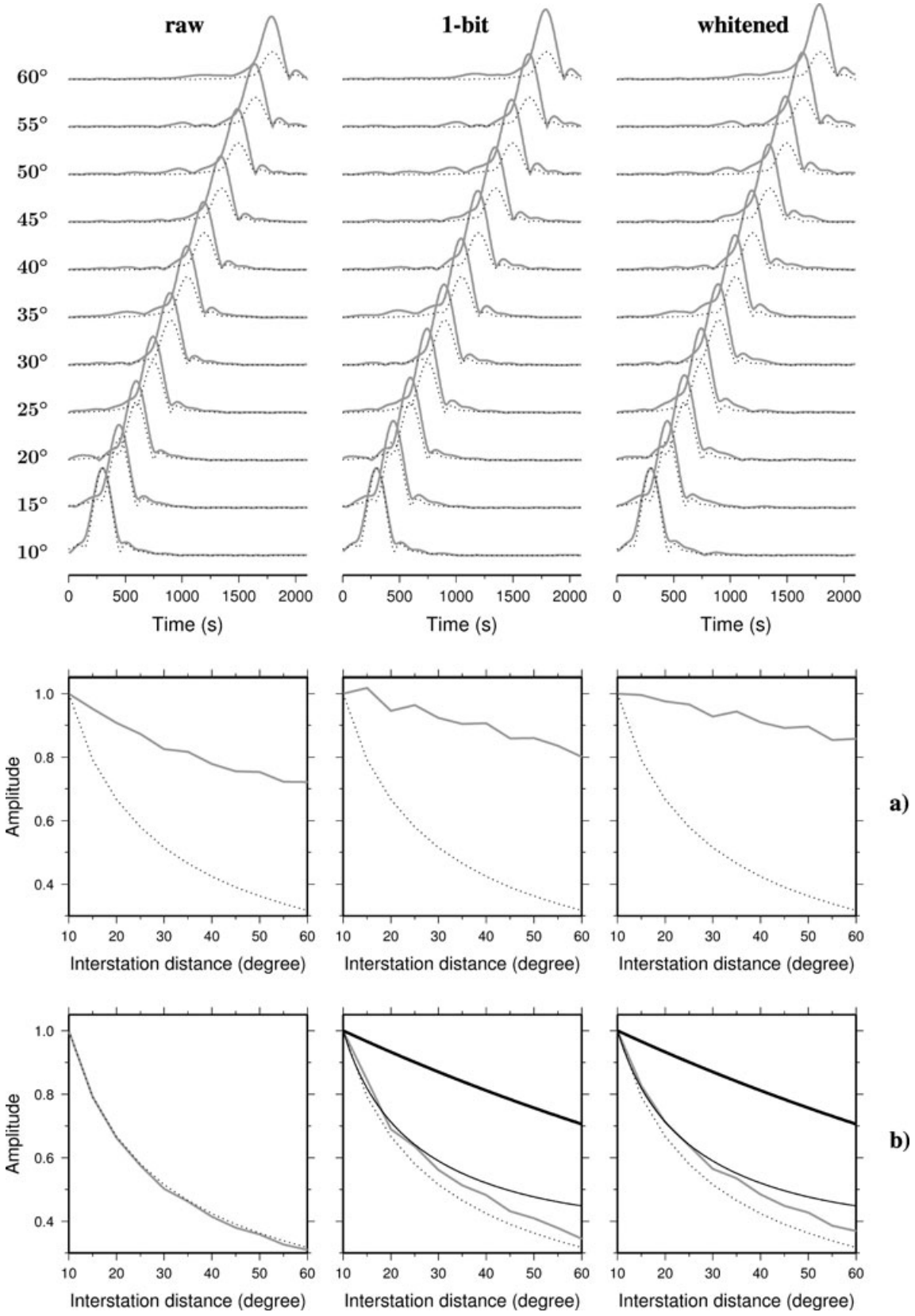

Figure 14. Comparison of the amplitude decay of the correlations envelope (grey line) with their corresponding fundamental mode (dotted line) in the case of noise sources distributed in a small patch. Top panel: Waveforms from the three processes (column) and all the stations (row) are presented. Bottom panel: (a) The maximum of amplitude is plotted as a function of interstation distance. (b) A geometrical correction is applied to the correlations. The decay of the raw noise correlation then fits the decay of the fundamental mode whereas the one-bit and the whitened noise correlations do not fit any decays (geometrical and intrinsic attenuations of the fundamental mode are plotted using thin and thick black lines, respectively.)

Rayleigh wave. These decays require further study to be properly interpreted.

Our results are consistent with previous studies. Larose *et al.* (2007) generates noise using a can of compressed air sprayed on the surface of a plexiglass plate. The amplitude of the correlations they acquire from an array of sensors starting at the air-jet source fits the amplitude of waveforms obtained from an active experiment. This is no longer true when frequency whitening is performed. Furthermore, the analysis of a seismic prospecting data set by Gouédard *et al.* (2008) shows that geometrical spreading retrieved by correlating direct waves (i.e. non-scattered waves) depends on the position of the sources. This observation indicates that the distribution of noise sources has to be known to measure the attenuation of the Earth from noise correlations. At present, our knowledge of this distribution is too poor, but we think that it will be greatly improved as localization of microseismic noise sources becomes a topic of intense research (e.g. Gerstoft & Tanimoto 2007; Kedar *et al.* 2008; Gerstoft *et al.* 2008).

A first important limitation in our experiment is that we do not have any incoherent noise (such as local or acquisition-related noise) or non-stationary phases (such as earthquakes) in our synthetics. These signals are often present in real data and can affect the amplitude of the correlations. Including such signals in our simulation could change our results. For instance, Figs 3 and 4 show that the number of realizations needed to get a stable error is larger for the one-bit than for the raw and the whitened noise correlation. This is the opposite of what is observed in practice in real data (e.g. Larose *et al.* 2004) because the one-bit normalization is usually employed to process incoherent noise or non stationary phases. As we have no such signals in our experiment, we do not take advantage of this process and just lose information, making the convergence slower.

In this work, the ratio of interstation distance to wavelength ranges from 2 to 15, as is the case for the ratio involved in correlations of real seismic noise. For this reason, we believe that our results are valid when using real seismic records. Nevertheless, our numerical experiment has a second important limitation: it involves long-period surface waves in a 1-D model whereas real seismic noise mostly propagates at high frequency (0.05–0.2 Hz) and therefore is very sensitive to strong 3-D structures present in the crust. Such structures scatter the incident wavefield and become secondary noise sources, making the distribution much more uniform and the wavefield much more equipartitioned than in the 1-D case (Hennino *et al.* 2001; Gouédard *et al.* 2008). Because of this phenomenon, the attenuation of the Earth may be easier to recover from noise correlations without knowing the precise location of the primary sources (Matzel 2008; Prieto *et al.* 2009). The great potential of these data in investigating the interior of the Earth is confirmed, although significant effort is still needed to improve our understanding and better extract useful attenuation constraints.

ACKNOWLEDGMENTS

The authors thank Laurent Stehly, Vedran Lekic, Barbara Romanowicz, Jean-Paul Montagner and Nikolaï M. Shapiro for fruitful discussions. The authors also thank two anonymous reviewers for comments that helped to improve the paper. We are grateful to the *Service de Calcul Parallèle* of the IPGP and to David Weissenbach for his help in the implementation of our code on the EGEE grid.

REFERENCES

Aki, K. & Richards, P., 1980. *Quantitative Seismology: Theory and Methods.* Freeman, San Francisco.

Bensen, G.D., Ritzwoller, M.H., Barmin, M.P., Levshin, A.L., Lin, F., Moschetti, M.P., Shapiro, N.M. & Yang, Y., 2007. Processing seismic ambient noise data to obtain reliable broad-band surface wave dispersion measurements. *Geophys. J. Int.,* **169,** 1239–1260, doi:10.1111/j.1365-246X.2007.03374.x.

Bensen, G.D., Ritzwoller, M.H., Barmin, M.P., Levshin, A.L., Lin, F., Moschetti, M.P., Shapiro, N.M. & Yang, Y., 2008. Broad-band ambient noise surface wave tomography across the united states. *J. geophys. Res.,* **113,** B05306, doi:10.1029/2007JB005248.

Campillo, M. & Paul, A., 2003. Long-range correlations in the diffuse seismic coda. *Science*, **299,** 547–549.

Cho, K., Herrmann, R.B., Ammon, C.J. & Lee, K., 2007. Imaging the upper crust of the korean peninsula by surface-wave tomography. *Bull. seism. Soc. Am.*, **67,** 198–207.

Colin de Verdière, Y., 2006. Mathematical models for passive imaging, I: general background, http://arxiv.org/abs/math-ph/0610043/.

Derode, A., Larose, E., Tanter, M., de Rosny, J., Tourin, A., Campillo, M. & Fink, M., 2003. Recovering the Green's function from field-field correlations in an open scattering medium (L). *J. acoust. Soc. Am.*, **113,** 2973–2976.

Duvall, T.L., Jefferies, S.M., Harvey, J. & Pomerantz, M.A., 1993. Time-distance helioseismology. *Nature*, **362,** 430–432.

Dziewonski, A.M. & Anderson, D.L., 1981. Preliminary reference Earth model. *Phys. Earth planet. Inter.*, **25,** 297–356.

Friedrich, A., Krüger, F. & Klinge, K., 1998. Ocean-generated microseismic noise located with the Gräfenberg array. *J. Seismol.*, **2,** 47–64.

Gerstoft, P. & Tanimoto, T., 2007. A year of microseisms in southern california. *Geophys. Res. Lett.,* **34,** L20304, doi:10.1029/2007GL031091.

Gerstoft, P., Shearer, P.M., Harmon, N. & Zhang, J., 2008. Global P, PP, and PKP wave microseisms observed from distant storms. *Geophys. Res. Lett.,* **35,** L23307, doi:10.1029/2008GL036111.

Gouédard, P., Roux, P., Campillo, M. & Verdel, A., 2008. Convergence of the two-points correlation function toward the Green's function in the context of a prospecting dataset. *Geophysics*, **73**(6), V47–V53.

Harmon, N., Gerstoft, P., Rychert, C.A., Abers, G.A., de la Cruz, M.S. & Fischer, K.M., 2008. Phase velocities from seismic noise using beamforming and cross correlation in costa rica and nicaragua. *Geophys. Res. Lett.,* **35,** L19303, doi:10.1029/2008GL035387.

Hennino, R., Tégourès, N., Shapiro, N.M., Margerin, L., Campillo, M., van Tiggelen, B. & Weaver, R., 2001. Observation of equipartition of seismic waves. *Phys. Rev. Lett.*, **85**(15), 3447–3450.

Kedar, S. & Webb, F.H., 2005. The ocean's seismic hum. *Science*, **307,** 682–683.

Kedar, S., Longuet-Higgins, M., Webb, F., Graham, N., Clayton, R. & Jones, C., 2008. The origin of deep ocean microseisms in the North Atlantic Ocean. *Proc. R. Soc. A*, **464,** 777–793.

Larose, E., Derode, A., Campillo, M. & Fink, M., 2004. Imaging from one-bit correlations of wide-band diffuse wavefields. *J. Appl. Phys.*, **95**(12), 8393–8399.

Larose, E., Roux, P. & Campillo, M., 2007. Reconstruction of Rayleigh-Lamb dispersion spectrum based on noise obtained from an air-jet forcing. *J. acoust. Soc. Am.,* **122**(6), 3437–3444.

Lin, F., Ritzwoller, M.H., Townend, J., Savage, M. & Bannister, S., 2007. Ambient noise Rayleigh wave tomography of New Zealand. *Geophys. J. Int.,* **170,** 649–666, doi:10.1111/j.1365-246X.2007.03414.x.

Lin, F., Moschetti, M.P. & Ritzwoller, M.H., 2008. Surface wave tomography of the western United States from ambient seismic noise: Rayleigh and Love wave phase velocity maps. *Geophys. J. Int.,* **173,** 281–298, doi:10.1111/j1365-246X.2008.03720.x.

Lobkis, O.I. & Weaver, R.L., 2001. On the emergence of the Green's function in the correlation of a diffuse field. *J. acoust. Soc. Am.*, **110,** 3011–3017.

Longuet-Higgins, M.S., 1950. A theory on the origin of microseisms. *Phil. Trans. R. Soc. Lond., A.*, **243,** 1–35.

Matzel, E., 2008. Attenuation tomography using ambient noise correlation. *Seism. Res. Lett.,* **79**(2), 358.

Nawa, K., Suda, N., Fukao, Y., Sato, T., Aoyama, Y. & shibuya, K., 1998. Incessant excitation of the Earth's free oscillations. *Earth. planet. Space*, **50,** 3–8.

Nishida, K. & Fukao, Y., 2007. Source distribution of Earth's background free oscillations. *J. geophys. Res.,* **112,** B06306, doi:10.1029/2006JB004720.

Paul, A., Campillo, M., Margerin, L., Larose, E. & Derode, A., 2005. Empirical synthesis of time-asymmetrical green functions from the correlation of coda waves. *J. geophys. Res.,* **110,** B08302, doi:10.1029/2004JB003521.

Prieto, G.A., Lawrence, J.F. & Beroza, G.C., 2009. Anelastic Earth structure from the coherency of the ambient seismic field. *J. geophys. Res.,* **144,** B07303, doi:10.1029/2008JB006067.

Rhie, J. & Romanowicz, B., 2004. Excitation of Earth's incessant free oscillations by atmosphere-ocean-seafloor coupling. *Nature*, **431,** 552–556.

Roux, P., Sabra, K.G. & Kuperman, W.A., 2005. Ambient noise cross-correlation in free space: Theoretical approach. *J. acoust. Soc. Am.,* **117**(1), 79–84, doi:10.1121/1.1830673.

Sánchez-Sesma, F.J. & Campillo, M., 2006. Retrieval of the Green's function from cross-correlation: the canonical elastic problem. *Bull. seism. Soc. Am.*, **96,** 1182–1191.

Sánchez-Sesma, F.J., Pérz-Ruiz, J., Campillo, M. & Lúzon, F., 2006. Elastodynamic 2D Green function retrieval from cross-correlation: canonical inclusion problem. *Geophys. Res. Lett.,* **33,** L13305, doi:10.1029/2006GL026454.

Sánchez-Sesma, F.J., Pérz-Ruiz, J., Lúzon, F., Campillo, M. & Rodrìguez-Castellanos, A., 2008. Diffuse fields in dynamic elasticity. *Wave Motion*, **45,** 641–654.

Shapiro, N.M. & Campillo, M., 2004. Emergence of broadband Rayleigh waves from correlations of the ambient seismic noise. *Geophys. Res. Lett.,* **31,** L07614, doi:10.1029/2004GL019491.

Shapiro, N.M., Campillo, M., Stehly, L. & Ritzwoller, M.H., 2005. High-resolution surface wave tomography from ambient seismic noise. *Science*, **307,** 1615–1618.

Snieder, R., 2004. Extracting the Green's function from the correlation of coda waves: a derivation based on stationary phase. *Phys. Rev. E,* **69,** 046610.

Snieder, R., 2007. Extracting the green's function of attenuating heterogeneous media from uncorrelated waves. *J. acoust. Soc. Am.*, **121,** 2637–2643.

Stehly, L., Campillo, M. & Shapiro, N., 2006. A study of the seismic noise from its long-range correlation properties. *J. geophys. Res.,* **111,** B10306, doi:10.1029/2005JB004237.

Stehly, L., Campillo, M. & Shapiro, N., 2007. Traveltime measurements from noise correlation: stability and detection of instrumental time-shifts. *Geophys. J. Int.,* **171,** 223–230, doi:10.1111/j.1365-246X.2007.03492.x.

Stehly, L., Fry, B., Campillo, M., Shapiro, N., Guilbert, J., Boschi, L. & Giardini, D., 2009. Tomography of the alpine region from observations of seismic ambient noise. *Geophys. J. Int.,* **178,** 338–350, doi:10.1111/j.1365-246X.2009.04132.x.

van Tiggelen, B.A., 2003. Green function retrieval and time-reversal in a disordered world. *Phys. Rev. Lett.,* **91**(24), 243904–4.

Wapenaar, K., 2004. Retrieving the elastodynamic Green's function of an arbitrary inhomogeneous medium by cross-correlation. *Phys. Rev. Lett.,* **93,** 254301–4.

Weaver, R.L. & Lobkis, O.I., 2001. Ultrasonics without a source: thermal fluctuation correlation at MHz frequencies. *Phys. Rev. Lett.,* **87,** 134301–4.

Weaver, R.L. & Lobkis, O.I., 2003. Elastic wave thermal fluctuations, ultrasonic waveforms by correlation of thermal phonons. *J. acoust. Soc. Am.,* **113,** 2611–2621, doi:10.1121/1.1564017.

Weaver, R.L., Froment, B. & Campillo, M., 2009. On the correlation of non-isotropically distributed ballistic scalar diffuse waves. *J. acoust. Soc. Am.*, **126,** 1817–1826.

Woodhouse, J.H. & Girnius, T.P., 1982. Surface waves and free oscillations in a regionalized earth model. *Geophys. J. R. astr. Soc.*, **78,** 641–660.

Yang, Y., Ritzwoller, M.H., Levshin, A.L. & Shapiro, N.M., 2007. Ambient noise Rayleigh wave tomography across europe. *Geophys. J. Int.*, **168,** 259–274.

Yao, H. & van der Hilst, R.D., 2009. Analysis of ambient noise energy distribution and phase velocity bias in ambient noise tomography, with application to SE Tibet. *Geophys. J. Int.*, **179,** 1113–1132.

Yao, H., van der Hilst, R.D. & de Hoop, M.V., 2006. Surface-wave array tomography in SE Tibet from ambient seismic noise and two-station analysis – I. Phase velocity maps. *Geophys. J. Int.,* **166,** 732–744, doi:10.1111/j.1365-246X.2006.03028.x.